# Comparison of Hippocalcin Translocation and Minor Phospholipid Distribution

Dana BIRUK <sup>1</sup>, Oleksandra FEDCHENKO <sup>23</sup>, Yevhenii SHEREMET <sup>23</sup>, Borys OLIFIROV <sup>23</sup>

1) Department of Biomedicine and Neuroscience, Kyiv Academic University, Kyiv, Ukraine E-mail: d.biruk@kau.edu.ua
ORCID: https://orcid.org/0009-0001-9812-1040

2) Department of Biophysics of Sensory Signaling, Bogomoletz Institute of Physiology of NAS of Ukraine, Kyiv, Ukraine

E-mail: bolifirov@biph.kiev.ua

ORCID: https://orcid.org/0000-0001-9915-7769

3) Laboratory of Molecular Assays and Imaging, Institute of Bioorganic Chemistry of PAS, Poznań, Poland

Received April 20, 2025, in the final form June 7, 2025 https://doi.org/10.3842/confKAU.2025.biol.01

> **Abstract.** Calcium ions (Ca<sup>2+</sup>) serve as vital second messengers in neurons, regulating numerous physiological processes. Neuronal calcium sensor (NCS) proteins play a key role in this regulation by detecting changes in Ca<sup>2+</sup> concentration in the cytosol and triggering downstream signalling. One such sensor, hippocalcin (HPCA), binds Ca<sup>2+</sup> and undergoes a reversible translocation to membranes, interacting with target proteins. Previous in vitro studies suggest that this translocation may be selective for membrane regions enriched with phosphatidylinositol 4,5-bisphosphate (PIP<sub>2</sub>) [Biochem. J. **391** (2005), 231–238]. To further investigate this issue, we analysed the translocation of fluorescently-tagged HPCA in HEK 293 cells following a rapid homogeneous increase in  $[Ca^{2+}]_i$  induced by photolysis of caged Ca<sup>2+</sup>. In a separate series of experiments, we also recorded the distribution of PIP<sub>2</sub> between the plasma membrane (PM) and intracellular membranes (IMs) using the fluorescently tagged PH domain of phospholipase C, which has a high affinity for PIP<sub>2</sub>. Despite substantial variability in PIP<sub>2</sub> localisation between PM and IMs in different cells, we found that PIP<sub>2</sub> is generally more enriched in the intracellular membranes rather than in the plasma membrane. Notably, HPCA did not show a consistent preference for either compartment. These findings suggest that other unidentified factors contribute to the translocation and membrane targeting of HPCA.

Keywords: hippocalcin; neuronal calcium sensors; PIP2; minor phospholipids.

### 1 Introduction

Calcium signalling processes demonstrate remarkable sensitivity to even minor fluctuations in cytosolic  $Ca^{2+}$  concentration ( $[Ca^{2+}]_i$ ). Notably, various types of  $Ca^{2+}$  signals might differ spatially, temporally, and in magnitude. Despite extensive research, numerous calcium-dependent mechanisms, such as those involved in neuronal plasticity that require precise and rapid regulation of neural activity, remain incompletely understood.

Neuronal Ca<sup>2+</sup> sensor (NCS) proteins, including NCS1, VILIP-1, HPCAL4, HPCAL1, hip-pocalcin, neurocalcin, recoverin, GCAPs, and KChIPs, may provide essential insights into these mechanisms. They act as cytosolic Ca<sup>2+</sup> binding proteins that transduce signals to downstream targets, playing critical roles in neuronal function. NCS proteins, despite sharing 22–55% sequence identity, exhibit highly diverse and non-overlapping physiological functions [6]. For instance, a knockout of neuronal calcium sensor-1 (NCS-1) in mice leads to increased dendritic

arbour complexity in the frontal cortex and a reduction in long-term potentiation (LTP) in the dentate gyrus [12].

Among the neuronal calcium sensor proteins, hippocalcin (HPCA) is particularly interesting due to its unique biophysical properties. Unlike some other NCS proteins, HPCA functions as a  $Ca^{2+}$ -dependent switch. At basal  $[Ca^{2+}]_i$  levels, the hydrophobic myristoyl group of HPCA is hidden. The Ca<sup>2+</sup> binding provoke conformational changes and expose the myristoyl group, allowing protein to associate with membranes. HPCA relies on N-terminal myristoylation for membrane association. HPCA was initially identified in the hippocampal pyramidal layer [9] and later found to be almost exclusively expressed in the central nervous system (CNS), with the highest expression levels in the hippocampus, cortex, striatum, and cerebellum [2]. Notably, among all analysed NCS proteins, HPCA exhibits the highest sensitivity to Ca<sup>2+</sup>, reaching its active state at the lowest Ca<sup>2+</sup> concentration [1]. Regarding the functional role of HPCA, it has been shown to mediate calcium signalling and regulate slow afterhyperpolarisation (sAHP) channels. Brief depolarizations sufficient to activate the sAHP in wild-type mice fail to elicit the sAHP in HPCA knockout mice [19]. Beyond its physiological role, HPCA mutations have been linked to neurological disorders. Specifically, mutations in the HPCA gene are associated with the orphan movement disorder known as autosomal recessive primary isolated dystonia (DYT2) [2, 14]. Additionally, it was shown that HPCA is implicated in cognitive functions, namely spatial and associative memory processes [8].

One of the most notable functional roles of HPCA identified so far is its involvement in NMDAR-dependent LTD, which is induced by a reduction in the number of AMPA receptors (AMPARs) on the postsynaptic membrane via clathrin-mediated endocytosis [15]. This process occurs in specialised postsynaptic structures called endocytic zones (EZs), which are enriched in the phospholipid Phosphatidylinositol-4,5-bisphosphate PIP<sub>2</sub>, a key regulator of clathrinmediated endocytosis. Beyond its role in endocytosis, PIP<sub>2</sub> also regulates phagocytosis, cell motility, signal transduction, and ion channel activity. PIP<sub>2</sub> is one of the polyphosphoinositides (PPIs), a group of essential minor phospholipids located in the inner leaflet of eukaryotic cell membranes, constituting approximately 1% of plasma membrane phospholipids [3, 17]. HPCA exhibits a high-affinity interaction with PIP<sub>2</sub>-containing membranes, suggesting that PIP<sub>2</sub> may influence its subcellular localisation and function [13]. However, whether this minor phospholipid is necessary for its membrane insertion remains unclear. These findings suggest that HPCA may play a critical role in key neuronal activity mechanisms, where even a small amount of this protein in the plasma membrane can significantly impact neuronal function. Such effects may become even more pronounced under pathological conditions, where  $[Ca^{2+}]_i$  fluctuate abnormally, further supporting the potential involvement of HPCA in neurodegenerative diseases.

#### 2 Methods

#### 2.1 HEK 293 cells

Human embryonic kidney (HEK) 293 cells were obtained from the Cell Culture Bank of the National Academy of Sciences of Ukraine (Bogomoletz Institute of Physiology, Kyiv, Ukraine). Cells were grown on the cell culture dish in Dulbecco's modified Eagle's medium (DMEM, Thermo Fisher Scientific, USA), supplemented with 10% fetal bovine serum (FBS, Thermo Fisher Scientific, USA) and 0.25% gentamicin (10 mg/ml stock solution) at 37 °C and 5%  $\rm CO_2$  in an atmosphere. The culture medium was changed every 3–5 days, and the cells were transfected 2–3 days after plating. Registration was performed using a confocal microscope 1–2 days after transfection.

#### 2.2 Transient transfection

The two-component Lipofectamine 3000 reagent (Thermo Fisher Scientific, USA) was used for transfection. All procedures were performed according to the protocols and recommendations provided by the manufacturer. The amount of DNA for transfection of one dish was 0.5  $\mu g$  for each plasmid construction. HEK 293 cells were co-transfected with a plasmid encoding HPCA tagged with the bright, photostable, and rapidly maturing fluorescent protein mBaoJin (HPCA-mBaoJin) [24]. In a second series of experiments, cells were co-transfected with yellow fluorescent protein fused with a neuromodulin C-terminal domain, a non-specific tag that evenly distributed across all membranes (EYFP-Mem) [10] and a cyan fluorescent protein fused to the pleckstrin homology domain of phospholipase  $\delta 1$  (PHD-ECFP), which binds PIP<sub>2</sub> with high affinity [11]. Cells were used for experiments 1–2 days post-transfection.

#### 2.3 Photolysis-induced calcium release

Nitrophenyl-EGTA (NP-EGTA; Thermo Fisher Scientific Inc., USA), a photolabile derivative of the calcium chelator EGTA, was used to increase  $[Ca^{2+}]_i$ . Exposure to short-wavelength radiation induces photolysis of the compound, enabling controlled  $Ca^{2+}$  release in individual cells by modulating the exposure time and photostimulation area.

#### 2.4 Confocal microscopy

Fluorescence images of a single focal plane were acquired using an Olympus FluoView FV1000 confocal laser scanning microscope (Olympus, Japan) at the Core Facilities of the National Academy of Sciences of Ukraine, Bogomoletz Institute of Physiology of NAS of Ukraine. The microscope was controlled via FV10-ASW software provided by the manufacturer. Images were acquired using a high-aperture water-dipping objective (60×NA 1.00, Olympus, Japan). HPCA-mBaoJin was excited using the 488 nm line of an argon laser, with emission collected within a 497–535 nm bandwidth. NP-EGTA was photolysed using a short wavelength semiconductor laser with a 405 nm emission line. A single photostimulation event was applied to the entire cell area within a frame, with a laser power of 20–25% and an exposure time of 8 ms per pixel. Microscopic image processing was performed using napari, enhanced with the domb-napari plugin and specialised Python libraries (NumPy, pandas, and Matplotlib) [4,5,21]. The source code for the custom-developed scripts is available in an open-access repository and published under open-source license (https://github.com/danabiruk/HPCA\_PIP2).

#### 2.5 Statistical methods

To assess the relationship between the maximal translocation of HPCA-mBaoJin we used linear regression models and the Bland–Altman plot. We employed probability density functions (PDFs) for the ratio between PHD-ECFP and EYFP-Mem to compare PIP<sub>2</sub> distributions across plasma and intracellular membranes. We confirmed significant differences in PIP<sub>2</sub> distributions between distinct cellular membrane pools using the Kolmogorov–Smirnov (KS) test. For the asymmetrical and unusual PIP<sub>2</sub> distributions in PM ROIs, we additionally applied a Gaussian mixture model (GMM) to check for distinct clusters within the distributions. This approach allowed us to analyze the distribution patterns and confirm the presence of significant differences. All calculations and analyses were performed in Python using the NumPy, SciPy, Scikit-learn, Seaborn, and Matplotlib libraries [4,5,16,20,22]. The source code for the statistical analysis is available in an open-access repository and published under open-source license (https://github.com/danabiruk/HPCA\_PIP2).

## 3 Data analysis and results

At basal intracellular calcium concentrations, HPCA primarily behaves as a cytoplasmic protein [18]. At the same time, in all investigated cells some dim intracellular regions were detected (Figure 1 (Aa), intracellular regions with low fluorescence intensity highlighted with dashed line). Notably, these intracellular regions, which initially exhibited lower HPCA fluorescence intensity, showed an increase in fluorescence following photolysis-induced Ca<sup>2+</sup> release (Figure 1 (Ab), the same region highlighted with Figure 1 (Aa)). This was strong evidence of HPCA insertions in intracellular membranes (IMs), most likely those of organelles, which are isolated from HPCA-mBaoJin diffusion from the cytoplasm. For a more accurate visualisation of the IMs, we introduced an intensity adjustment to the images before the photolysis-induced Ca<sup>2+</sup> release. Subtraction of the averaged cytoplasmic intensity significantly increased the contrast of the membrane-bound intracellular compartments that may be diffusionally isolated. The cytoplasmic intensity was estimated as the averaged signal intensity in the regions between the cell border and the dim intracellular regions that were visually detected. On adjusted images, IMs exhibit a complex structure with multiple isolated compartments, as shown in Figure 1 (B) (the highlighted region is the same as Figure 1 (A)).

A differential imaging approach was used to quantify HPCA translocation dynamics in response to photolysis-induced  $Ca^{2+}$  release. This method enabled the detection of fluorescence intensity changes over time, allowing for the identification of regions associated with HPCA insertions. Fluorescence redistribution was determined by comparing pixel intensity changes across sequential frames, with regions of increased fluorescence appearing in red and decreased fluorescence in green in pseudo-colour images [14]. HPCA translocation regions were detected on differential images that demonstrate massive areas across the PM (indicated with white arrows in Figure 1(C)), and distinct punctate regions within the cytoplasm (highlighted in Figure 1(C)). As expected, the intracellular translocation regions in the differential images confidently overlap with previously detected intracellular compartments (Figure 1(C), the highlighted region is the same as Figure 1(A) and (B)). According to these observations, the separated regions of interest (ROIs) for PM and IMs translocation sites were used for further analysis.

For all cells investigated (n=12), in response to photolysis-induced  $\operatorname{Ca}^{2+}$  release relative fluorescence changes  $(\Delta F/F_0)$  in total translocation sites for red increased sites (red trace in Figure 1 (D)) were accompanied by green decreased sites in the cytoplasm (green trace in Figure 1 (D)), and average fluorescence changes across the whole cell (white contour in Figure 1 (C) and blue trace in Figure 1 (D)) were negligible, indicating that a total amount of HPCA-mBaoJin was preserved.

Unfortunately, due to inherent differences in initial fluorescence intensities  $(F_0)$  between translocation sites on PM and IMs, comparison of the relative fluoroscence intesity changes  $(\Delta F/F_0)$  was not applied. Instead, to compare translocation amplitudes between PM and IMs, intensity changes were expressed as  $\Delta F - F_0$ . This value expresses the difference between the absolute intensity changes  $\Delta F$  immediately after the photolysis-induced  $\operatorname{Ca}^{2+}$  release, indicated by the dashed line in Figure 1 (D)  $(t=10~\mathrm{s})$  and the average initial intensity  $F_0$  before the  $\operatorname{Ca}^{2+}$  release  $(t=0-8~\mathrm{s})$ .

Regression analysis assessed the relationship between the maximal translocation of HPCA to PM and IMs regions and showed a strong linear dependence (Figure 1 (E),  $R^2 = 0.945$ ) and the regression slope was not significantly different from 1 (one-sample t-test, p = 0.381), indicating that HPCA translocation amplitudes were the same without preference for both region types. Observed even distribution on the Bland–Altman plot (Figure 1 (F), 95% confidential interval -42.8...54.3 a.u.) and mean differences between the maximum translocation amplitudes of only 5.8 a.u.  $\pm 24.8$  also supported the reliability of our measurements.

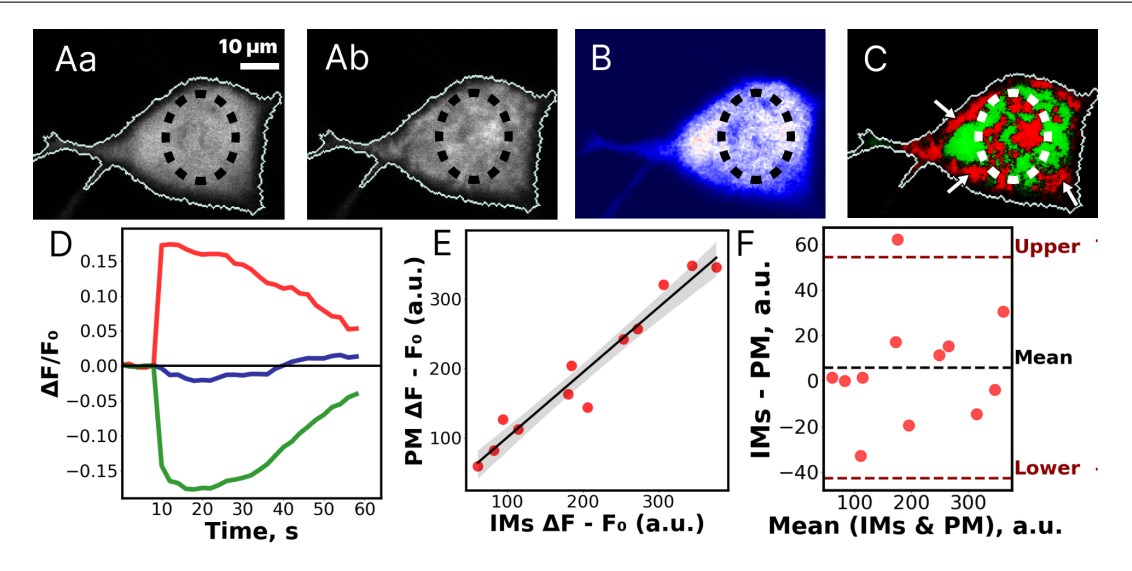


Figure 1. HPCA translocation shows no regional preference in HEK 293 cells. (A) Fluorescence image showing HPCA distribution before (Aa) and redistribution after photolysis-induced Ca<sup>2+</sup> release (Ab). (B) Subtraction of the averaged cytoplasmic intensity before photolysis-induced Ca<sup>2+</sup> release (C) Differential images showing HPCA translocations. The dashed line and arrows indicate the regions used for analysis. (D) Intensity profiles from regions where HPCA decreased (green), increased (red), and across the whole cell (blue). (E) Regression analysis of the relationship between the maximal translocation of HPCA to PM and IMs regions. (F) Bland–Altman analysis assessing the agreement between maximal HPCA translocation to PM and IMs.

To characterise the distribution of PIP<sub>2</sub> between different membrane pools, a further set of experiments was performed using the combination of the non-specific membrane tag EYFP-Mem and the PIP<sub>2</sub>-specific tag PHD-ECFP. By studying the co-distribution of the tags, we were able to directly observe the amount and distribution of PIP<sub>2</sub> in both PM and IMs sites.

EYFP-Mem was localised preferentially to the membranes (Figure 2 (A)), whereas a significant cytoplasmic fraction was observed for PHD-ECFP (Figure 2 (B)). The PH domain has a significant affinity not only for PIP<sub>2</sub>, but even higher for inositol triphosphate (IP<sub>3</sub>) [23], and a high cytoplasmic IP<sub>3</sub> concentration may be an unexpected feature of HEK cells causing the observed distribution of the tag.

Overlaying the EYFP-Mem and PHD-ECFP channels reveals numerous co-localisation sites throughout the PM (arrows and dashed line in Figure 2(C)) and in the cytoplasm (dashed line in Figure 2 (C)), and these distinct PM and IMs regions were selected for further analysis. To estimate the density of the PIP<sub>2</sub> distribution in the membranes, the dimensionsless pixel-wise ratio between PHD-ECFP and EYFP-Mem fluorescence intensities  $(I_{CFP}/I_{YFP})$  was calculated. Heterogeneity of PIP<sub>2</sub> density in PM regions is observed as substantial difference in  $I_{CFP}/I_{YFP}$ values, as shown in Figure 2(D), in which arrows indicate multiple sites of higher PIP<sub>2</sub> concentration. The pronounced asymmetry and multimodality of the  $I_{\rm CFP}/I_{\rm YFP}$  distribution in PM regions (orange in Figure 2(E)) motivated us to perform a Gaussian mixture model analysis. For the representative cell, four Gaussian components were detected according to the Bayesian information criterion (BIC), as shown in Figure 2 (F), indicating a highly heterogeneous distribution of PIP<sub>2</sub> across the PM. On the other hand, there are significantly higher median values of  $I_{\text{CFP}}/I_{\text{YFP}}$  in the IMs regions compared to PM ones (Figure 2(G), KS statistic = 0.6410, p < 0.001). Similar relationships were observed in all cells examined (see Table 1), without a clear relationship between PIP<sub>2</sub> density in PM and IMs  $(n = 7, \text{ Figure 2 (H)}, R^2 = 0.832)$  and the regression slope was significantly different from 1 (one-sample t-test, t = -3.842, p = 0.0121), indicating unequal distribution of PIP<sub>2</sub> between PM and IMs.

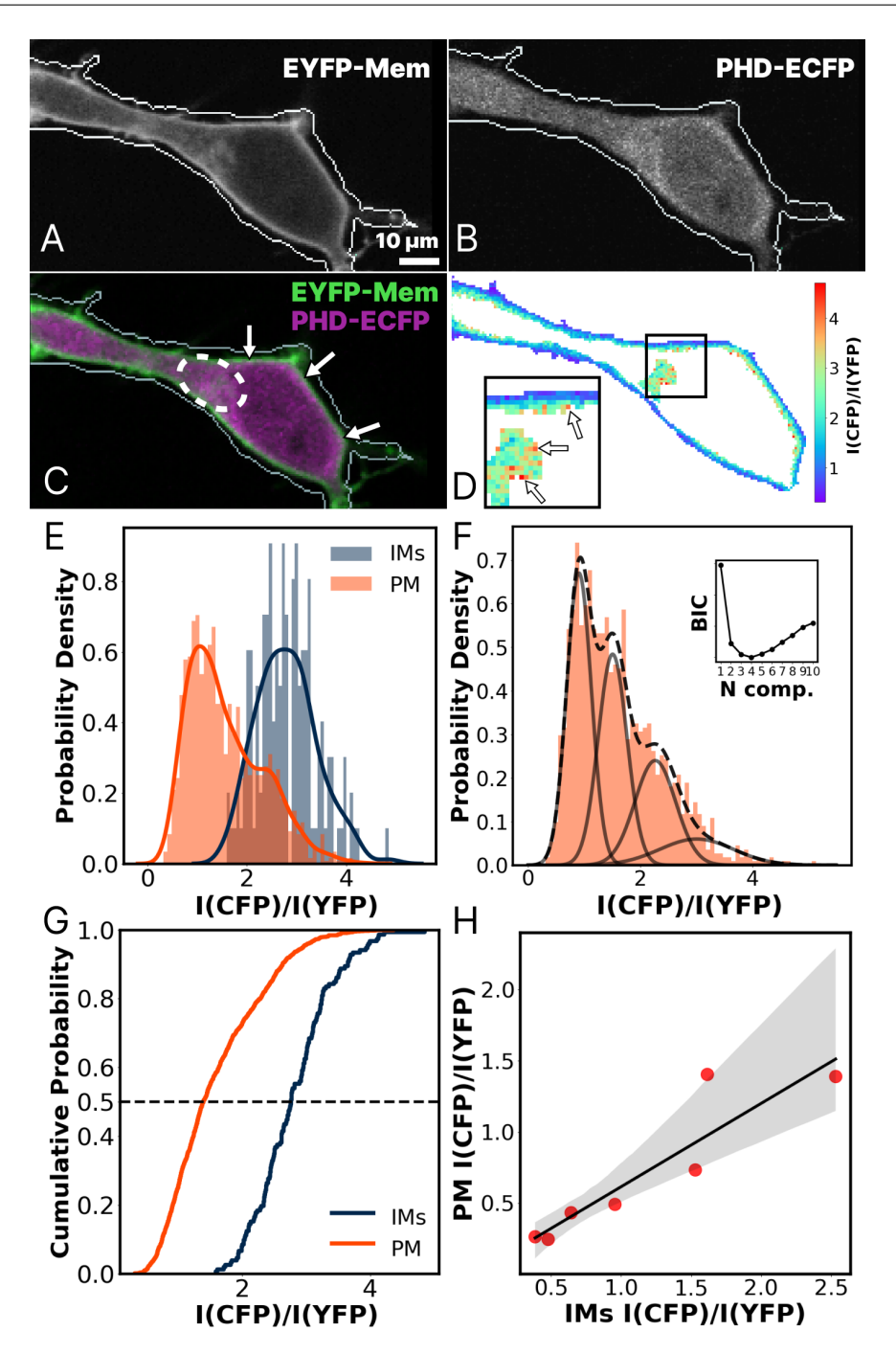


Figure 2. PHD-ECFP as a marker for comparative analysis of PIP<sub>2</sub> distribution between PM and IMs in HEK 293 cells. (A) Fluorescence image showing EYFP-Mem and (B) PHD-ECFP distribution. (C) Overlay of EYFP-Mem and PHD-ECFP images. Co-localisation is indicated by the white dashed line (cytoplasmic region) and white arrows (PM). (D) Pixel-wise ratio image showing the relative distribution of PHD-ECFP to EYFP-Mem fluorescence intensities. The black rectangle shows a zoomed-in area where red regions (highlighted by arrows) indicate sites with a high PHD-ECFP/EYFP-Mem ratio. (E) Probability density function (PDF) of the ratio of  $I_{\rm CFP}/I_{\rm YFP}$  in regions of interest (ROIs) corresponding to the PM (orange) and IMs (blue). (F) Gaussian mixture model (GMM) analysis of the ratio between  $I_{\rm CFP}/I_{\rm YFP}$  in the PM, based on Bayesian information criterion (BIC) optimisation shown in the insert. (G) Cumulative density function (CDF) of the ratio of  $I_{\rm CFP}/I_{\rm YFP}$  in regions of interest (ROIs) corresponding to the PM (orange) and IMs (blue). (H) Regression analysis of the median intensity ratios ( $I_{\rm CFP}/I_{\rm YFP}$ ) comparing PM and IMs for all studied cells.

PM	IMs	KS statistic, p-value
0.6405	0.4327	0.4104, < 0.001
0.3846	0.2662	0.3248, < 0.001
0.4767	0.2463	0.5178, < 0.001
2.5323	1.3893	0.6410, < 0.001
1.5274	0.7354	0.7350, < 0.001
1.6120	1.4071	0.2411, < 0.001
0.9527	0.4926	0.6394, < 0.001

**Table 1.** Median  $I_{\text{CFP}}/I_{\text{YFP}}$  ratios and KS test results for all examined cells.

## 4 Conclusions

Our findings indicate that, despite the highly variable distribution of PIP<sub>2</sub> between IMs and PM in different cells, with no consistent pattern, HPCA redistribution occurs without a clear preference for either the plasma or intracellular membranes. While HPCA exhibits affinity for PIP<sub>2</sub> [13], the observed redistribution pattern suggests that other factors may control its translocation from the cytosol to the membranes.

The cell-to-cell variability in PIP<sub>2</sub> distribution between IMs and PM may reflect dynamic changes in phospholipid biosynthesis and membrane composition during different stages of the cell cycle [7]. In contrast, the consistency of HPCA translocation implies that its signalling is likely regulated independently of these phospholipid dynamics.

Given the higher affinity of HPCA to  $Ca^{2+}$  in comparison to many other NCS proteins [1], its binding to PIP<sub>2</sub> might represent a key element of downstream signalling. However, the localisation of PIP<sub>2</sub> should depend on the specific membrane composition, suggesting the involvement of other regulatory components that may interact with both HPCA and PIP<sub>2</sub>.

Notably, PIP<sub>2</sub> can be hydrolysed by phospholipase C (PLC) into IP<sub>3</sub> and DAG. This process, like HPCA activation, is also calcium-dependent. Although both pathways are initiated by the increase in  $[Ca^{2+}]_i$ , they likely represent distinct pathways of  $Ca^{2+}$ -mediated signalling. Future studies examining how the spatial and temporal characteristics of  $Ca^{2+}$  signals influence HPCA redistribution may provide deeper insights into its functional role. It is also significant to consider potential competition between  $Ca^{2+}$  sensor proteins and the possible convergence of their downstream targets.

#### Acknowledgements

We are deeply grateful to our colleagues from the YPBiotech, R&D department of the YURiA-PHARM pharmaceutical group of companies. The Head of YPBiotech Mr. Oleksandr Hubar, biotechnologist Mr. Nazarii Hrubiian, and junior biotechnologist Ms. Anastasiia Romanenko for the design and assembly of the HPCA-mBaoJin plasmid vector.

#### Funding

This work was funded by the Long-term program of support of the Ukrainian research teams at the Polish Academy of Sciences, carried out in collaboration with the U.S. National Academy of Sciences with the financial support of external partners (PAN.BFB.S.BWZ.405.022.2023), the Ministry of Education and Science of Ukraine grant (0123U102767), and the National Academy of Science of Ukraine grant (0124U001556).

## References

- [1] Burgoyne R.D., Neuronal calcium sensor proteins: generating diversity in neuronal Ca<sup>2+</sup> signalling, *Nature Rev. Neurosci.* 8 (2007), 182–193.
- [2] Charlesworth G., Angelova P., Bartolomé-Robledo F. et al., Mutations in HPCA cause autosomal-recessive primary isolated dystonia, Amer. J. Human Genetics 96 (2015), 657–665.
- [3] Dickson E., Hille B., Understanding phosphoinositides: rare, dynamic, and essential membrane phospholipids, *Biochemical J.* **476** (2019), 1–23.
- [4] Harris C., Millman K., van der Walt S.J. et al., Array programming with NumPy, Nature 585 (2020), 357–362.
- [5] Hunter J.D., Matplotlib: A 2D graphics environment, Comput. in Sci. Eng. 9 (2007), 90–95.
- [6] Ikura M., Ames J., Genetic polymorphism and protein conformational plasticity in the calmodulin superfamily: Two ways to promote multifunctionality, Proc. Natl. Acad. Sci. USA 103 (2006), 1159–1164.
- [7] Jackowski S., Cell cycle regulation of membrane phospholipid metabolism, J. Biol. Chem. 271 (1996), 20219–20222.
- [8] Kobayashi M., Masaki T., Hori K. et al., Hippocalcin-deficient mice display a defect in cAMP response element-binding protein activation associated with impaired spatial and associative memory, *Neurosci.* **133** (2005), 471–484.
- [9] Kobayashi M., Takamatsu K., Saitoh S., Miura M., Noguchi T., Molecular cloning of hippocalcin, a novel calcium-binding protein of the recoverin family exclusively expressed in hippocampus, *Biochem. Biophys. Res. Com.* 189 (1992), 511–517.
- [10] Liu Y., Fisher D., Storm D., Intracellular sorting of neuromodulin (GAP-43) mutants modified in the membrane targeting domain, J. Neurosci. 14 (1994), 5807–5817.
- [11] Mashanov G., Tacon D., Peckham M., Molloy J., The spatial and temporal dynamics of pleckstrin homology domain binding at the plasma membrane measured by imaging single molecules in live mouse myoblasts, J. Biol. Chem. 279 (2004), 15274–15280.
- [12] Ng E., Georgiou J., Avila A. et al., Mice lacking neuronal calcium sensor-1 show social and cognitive deficits, Behavioural Brain Res. 381 (2020), 112420.
- [13] O'Callaghan D., Haynes L., Burgoyne R., High-affinity interaction of the N-terminal myristoylation motif of the neuronal calcium sensor protein hippocalcin with phosphatidylinositol 4,5-bisphosphate, *Biochem. J.* 391 (2005), 231–238.
- [14] Osypenko D., Dovgan A., Kononenko N. et al., Perturbed Ca<sup>2+</sup>-dependent signaling of DYT2 hippocalcin mutant as mechanism of autosomal recessive dystonia, Neurobiol. Disease 132 (2019), 104529.
- [15] Palmer C., Lim W., Hastie P. et al., Hippocalcin functions as a calcium sensor in hippocampal LTD, *Neuron* 47 (2005), 487–494.
- [16] Pedregosa F., Varoquaux G., Gramfort A. et al., Scikit-learn: Machine learning in Python, J. Machine Learning Res. 12 (2011), 2825–2830.
- [17] Rusinova R., Hobart E., Koeppe R., Andersen O., Phosphoinositides alter lipid bilayer properties, J. Gen. Physiol. 141 (2013), 673–690.
- [18] Sheremet Y., Olifirov B., Okhrimenko A., Cherkas V., Bagatskaya O., Belan P., Hippocalcin distribution between the cytosol and plasma membrane of living cells, *Neurophysiol.* **52** (2020), 2–13.
- [19] Tzingounis A., Kobayashi M., Takamatsu K., Nicoll R., Hippocalcin Gates the Calcium activation of the slow afterhyperpolarization in hippocampal pyramidal cells, *Neuron* **53** (2007), 487–493.
- [20] Virtanen P., Gommers R., Oliphant T.E. et al., SciPy 1.0: fundamental algorithms for scientific computing in Python, Nature Methods 17 (2020), 261–272.
- [21] McKinney W., Data structures for statistical computing in Python, in Proceedings of the 9th Python in Science Conference, Editors S. van der Walt and J. Millman, 2010, 56–61.
- [22] Waskom M.L., Seaborn: statistical data visualization, J. Open Source Software 6 (2021), 3021.
- [23] Wen Y., Vogt V.M., Feigenson G.W., PI(4,5)P<sub>2</sub> clustering and its impact on biological functions, Ann. Rev. Biochem. 90 (2021), 681–707.
- [24] Zhang H., Lesnov G., Subach O. et al., Bright and stable monomeric green fluorescent protein derived from StayGold, Nature Methods 21 (2024), 657–665.

## Порівняння транслокації гіпокальцину та розподілу мінорних фосфоліпідів

Дана БІРУК $^1$ , Олександра  $\Phi$ ЕДЧЕНКО $^{23}$ , Євгеній ШЕРЕМЕТ $^{23}$ , Борис ОЛІ $\Phi$ ІРОВ $^{23}$ 

1) Кафедра біомедицини та нейронаук, Київський академічний університет, Київ, Україна E-mail: d.biruk@kau.edu.ua ORCID: https://orcid.org/0009-0001-9812-1040

2) Відділ біофізіки сенсорної сигналізації, Інститут фізіології ім. О.О. Богомольця НАН України, Київ, Україна

E-mail: bolifirov@biph.kiev.ua

ORCID: https://orcid.org/0000-0001-9915-7769

3) Лабораторія молекулярного аналізу та візуалізації, Інститут біоорганічної хімії ПАН, Познань, Польща

Отримано 20 квітня 2025, у фінальній формі 7 червня 2025 https://doi.org/10.3842/confKAU.2025.biol.01

> **Анотація.** Іони кальцію (Ca<sup>2+</sup>) є ключовими вторинними месенджерами в нейронах, регулюючи низку важливих фізіологічних процесів. Білки родини нейрональних кальцієвих сенсорів (NCS) відіграють центральну роль у цій регуляції, реагуючи на зміни концентрації Ca<sup>2+</sup> у цитозолі та ініціюючи відповідні сигнальні каскади. Одним із таких білків є гіпокальцин (HPCA), який зв'язує  $\mathrm{Ca}^{2+}$  і здатен транслокуватись до клітинних мембран, де взаємодіє з білками-мішенями. Попередні in vitro дослідження продемонстрували, що ця транслокація може відбуватись вибірково до ділянок мембрани, збагачених фосфатидилінозитол-4,5-біфосфатом (PIP $_2$ ) [Biochem. J. **391** (2005), 231-238]. У нашому дослідженні ми проаналізували поведінку флуоресцентно міченого НРСА у клітинах НЕК 293 після швидкого й рівномірного підвищення внутрішньоклітинної концентрації  $\mathrm{Ca}^{2+}$ , індукованого фотолізом. Окремо було досліджено розподіл PIP<sub>2</sub> між плазматичною мембраною та внутрішньоклітинними мембранами за допомогою міченого РН-домену фосфоліпази С, який має високу афінність до PIP<sub>2</sub>. Попри значну варіабельність, у середньому більша кількість  $\mathrm{PIP}_2$  спостерігалась на внутрішніх мембранах. Водночас НРСА не демонстрував переваги до жодного з мембранних компартментів, що свідчить про участь додаткових, наразі неідентифікованих факторів у його взаємодії з мембранами.

> Ключові слова: гіпокальцин; нейрональні кальцієві сенсори, РІР2, мінорні фосфоліпіди.